ELSEVIER

Contents lists available at ScienceDirect

Chemical Physics Letters

journal homepage: www.elsevier.com/locate/cplett



Research paper



Thermal stability analysis of myoglobin based on native mass spectrometry and ultraviolet photodissociation

Pan Luo^{a,b,1}, Dai Zhang ^{a,c,1}, Jin Liu ^d, Yue Xuan ^a, Haoxin Fan ^{a,e}, Jieying Xue ^a, Zheyi Liu ^{a,e,**}, Fangjun Wang ^{a,e,*}

- a State Key Laboratory of Chemical Reaction Dynamics, Dalian Institute of Chemical Physics, Chinese Academy of Sciences, Dalian 116023, China.
- ^b Institute of Advanced Science Facilities, Shenzhen 518107, China.
- ^c University of Science and Technology of China, Anhui 230026, China.
- ^d Dalian Medical University, Dalian 116044, China
- e University of Chinese Academy of Sciences, Beijing 100049, China.

ARTICLE INFO

Keywords:

Native mass spectrometry (nMS) Ultraviolet photodissociation (UVPD) Thermal stability Molecular dynamics (MD) simulation

ABSTRACT

Thermal stability analysis of proteins awaits a residue-level elucidation of the structure–function relationships. Herein, we integrated native mass spectrometry (nMS) and 193-nm ultraviolet photodissociation (UVPD) to probe the relevant in-solution conformation dynamics of myoglobin (Mb) after heat treatment. The results demonstrated that heating at 50 $^{\circ}$ C or 75 $^{\circ}$ C induced the stabilization of the heme-binding pocket, and a His93-heme-His64 double coordination was formed at 75 $^{\circ}$ C, as seen by the reduced heme ion release. Molecular dynamics (MD) simulation further confirmed the MS results. Moreover, heating at 85 $^{\circ}$ C substantially disrupted the structural integrity of most protein, leading to a significant decline in MS signal.

1. Introduction

Characterization the protein structures with residue resolution are of great significance for understanding the structure–function relationships [1,2]. The thermal stability analysis of proteins requires efficient structural analysis methods to elucidate molecular mechanisms. Owing to the remarkable attributes of high sensitivity and conformational selectivity, an array of mass spectrometry (MS)-based approaches is high complementary to the conventional protein structure characterization techniques, X-ray crystallography and cryo-electron microscopy (cryo-EM) [3–6].

Different from the conventional bottom-up MS/MS analysis which analyze the abundance changes of tryptic peptides, another series of MS strategies realizes direct transfer of intact proteins or protein complexes into the gas phase by the advent of native mass spectrometry (nMS) employing nondenaturing electrospray ionization (nESI). nMS has been established as a critical platform for characterizing the in-solution protein dynamics, offering exceptional sensitivity, high-throughput capacity, and concurrent detection of multiple components within complex mixtures [3,5–8]. It has been reported that the tertiary structure of

protein is the key determinant of charge state distributions (CSDs) [9], the compact conformation commonly exhibited low charge states, while more charges could be grasped by extend conformation during native ESI process. Besides, the collision cross-section (CCS) obtained by ion mobility-MS (IM-MS) exams the overall size and shape of protein ions, but also lacks of residual information. To obtain the molecular details of protein structural changes, the native top-down MS (nTDMS) strategy utilizing the dissociation methods following MS1 analysis could provide sub-region and residue-level information of the protein conformation dynamics [10]. However, the common dissociation methods such collision-based methods or electron-based methods show less efficiency for fragmentation of native-like protein ions, resulting the limited structural information or low residue coverage [11-13]. Owing to the fast activation process and the property of retaining structureinformative noncovalent fragment ions, the integration of 193-nm ultraviolet dissociation (UVPD) with nMS have been shown to be an efficient strategy for probing the molecular details of protein conformational alterations, providing near complete coverage of residues [14-20].

In this study, we integrated nMS with 193-nm UVPD to

^{*} Corresponding author.

^{**} Corresponding author.

E-mail addresses: zy_liu@dicp.ac.cn (Z. Liu), wangfj@dicp.ac.cn (F. Wang).

¹ Those two authors contributed equally to this work.

comprehensively characterize the thermal stability and in-solution conformation dynamics of myoglobin (Mb). nMS can probe the integrity and overall structural changes of hemoprotein after heat treatment based on the CSDs. Results demonstrated the high thermal stability of Mb, which can maintain the majority of its tertiary structures after short-term heat treatment below the melting temperature (T_m). Then, the specific myoglobin-heme complex ions (hMb) with a charge state of 8+ sprayed from different solutions were isolated and subjected to 193-nm UVPD, which offered a sensitive approach to capture the molecular details in the heme-binding pocket. This strategy underscores the great potential of UVPD on precise elucidation of protein stability at residue level.

2. Method

2.1. Chemicals and reagents

Ammonium acetate (NH₄OAc), equine heart Mb, and other unspecified chemical reagents were purchased from Sigma Aldrich (St. Louis, MO). All deionized water used in the experiments was prepared using a Milli-O water purification system (Millipore, USA).

2.2. nMS and UVPD analysis

Prior to nMS and UVPD analysis, Mb was dissolved in deionized water with a concentration of 20 μ M, heated at 50 °C, 75 °C, or 85 °C for 3 min, cooled to room temperature, and then 1:1 (ν /v) mixed with 400 mM NH₄OAc to a final concentration of 10 μ M. The control group was directly dissolved in 200 mM NH₄OAc with a concentration of 10 μ M.

The Mb solution was directly infused into MS via a static ESI source operated with a spray voltage at $1.2~\rm kV$. All nMS and UVPD analyses were performed on an Orbitrap Fusion Lumos Tribrid mass spectrometer (Thermo Fisher, San Jose, CA, USA) equipped with a 193 nm ArF excimer laser (Gam laser, Orlando, FL, USA) as described in our previous works [17–19]. All mass spectra were collected at a mass resolution of 240 K by averaging 500 micro scans. The normalized AGC target (%) and maximum injection time (ms) of MS1 was set at 200, 200 while of MS2 was set at 1000, 200. All UVPD experiments were performed through activation by a single pulse of laser irradiation (5 ns, $1.5~\rm mJ$) and the MS2 data was collected with an isolation width of 2~m/z. Three replicates were performed for all experiments.

2.3. UVPD data analysis

The acquired UVPD raw files were successively converted to mzML format by MSConvert and deconvoluted by TopFD_GUI with an S/N ratio of 3 [21,22]. Using a custom R script, 12 UVPD fragment ion types including a, a + 1, a + 2, b, c, x, x + 1, y, y - 1, y - 2, z, and z + 1 ions with ± 2 ppm mass accuracy threshold were considered for database search. Fragment ions were filtered as confident identifications based on high repeatability (≥ 16 of 20 scans per replicate) and an isotope pattern similarity (Pearson correlation coefficient ≥ 0.7) between calculated and experimental patterns. Differential analysis between control and experimental groups were based on the common fragment ions that identified in both groups. The intensities of identified fragment ions were median normalized. Residue FYs were calculated by using the normalized intensities of all fragment ions [20].

2.4. Molecular dynamics simulation

Mb (PDB: 1dwr) was simulated in tip4pew water models using the ff19SB force fields with Amber22. We simulated the system positioned 15 Å from the boundary within a simulation box employing periodic boundary conditions. A steepest descent energy minimization was performed, followed NVT ensemble from 0 to 298 K and 348 K over 600 ps simulation period with CA atoms constrained, respectively. Initial

conditions for the 15 ns production simulations were taken from the final structures and velocities of the equilibration simulations. The simulations were conducted in the NPT ensemble at 1 atm, without any special mass repartitioning. SHAKE was applied to constrain bond lengths involving hydrogen atoms, and a simple coulomb term was managed to handle electrostatics. The cutoff for nonbinding interactions was set at 10~Å, and MD time step was 2~fs.

3. Results and discuss

3.1. nMS probes the overall structural changes

Investigating the thermal stability and elucidating the in-solution structural changes of Mb are critical for understanding their performance and potential applications. In this study, we employed nMS to assess the impact of thermal treatment on the structural integrity of hMb. Previous research has demonstrated that CSDs obtained in ESI-MS provide a reliable means for monitoring global protein structural changes. Specifically, proteins with compact conformation exhibit lower CSDs than those with extended conformation. The ESI mass spectrum of hMb ions under native-like conditions (200 mM NH₄OAc) is observed with CSDs ranging from 7+ to 9+, with 8+ being the most predominant (Fig. 1a). In the experimental groups, thermal treatments at 50 °C or 75 °C, have no observable impact on the CSDs of hMb (Fig. 1b, c), indicating that the compact tertiary structures are largely retained. However, when the temperature was increased to 85 °C, the CSDs of hMb remained largely unchanged, but a notable reduction in overall MS intensity was observed (Fig. 1d). This significant decrease in intensity was accompanied by the appearance of a small fraction of apomyoglobin (aMb), likely due to the unfolding and subsequent precipitation of a substantial portion of the protein. These observations are consistent with the previously reported T_m of hMb, as determined by IM-MS [23]. Therefore, nMS successfully monitored the structural stability of hMb following heat treatment at various temperatures. Our results demonstrate that the compact tertiary structure of hMb remains stable following short-term heat treatment below the T_m , while heating above the T_m leads to irreversible disruption of its three-dimensional structure.

3.2. 193-nm UVPD probes the structural details

As nMS primarily probes overall structural changes through CSDs, the observation that the three-dimensional structure of Mb remained almost unchanged after heat treatments at 50 °C or 75 °C prompted us to employ UVPD for further investigation into conformational changes at the residue- or secondary- structure level by the structure informative photofragments. Thus, we applied UVPD to explore the detailed conformation changes of *h*Mb⁸⁺ after 50 °C or 75 °C heating treatments (Fig. 2, 3). The resulting sequence coverages for the control group and each denaturation condition were comparable, each attaining approximately 90 %, thereby enabling detailed interrogations of hMb conformation with high residue coverage (Fig. 2a). Notably, the substantial differences in heme binding affinities were observed across the various denaturation treatments (Fig. 2b), indicating altered conformations of hMb⁸⁺ within the binding pocket. Specifically, heat treatment at 75 °C led to a significant increase in heme binding affinity, which was reflected by a 7.2 % decrease in the relative intensities of ejected heme ions in the UVPD spectra compared to the control group (without heat treatment). These findings suggest that, despite maintaining consistent charge states indicative of similar overall conformations, irreversible structural changes in the secondary structure of $h\mathrm{Mb}^{8+}$ occurred following heat treatments at different temperatures.

Then, detailed conformation changes at the residue level were analyzed by examining the changes of fragmentation yield (FY) in $h \text{Mb}^{8+}$ after different denaturation treatments (Fig. 3). Compared to the control group without heat treatment, the majority of the residues along the protein sequence showed significant FY increase but not induce

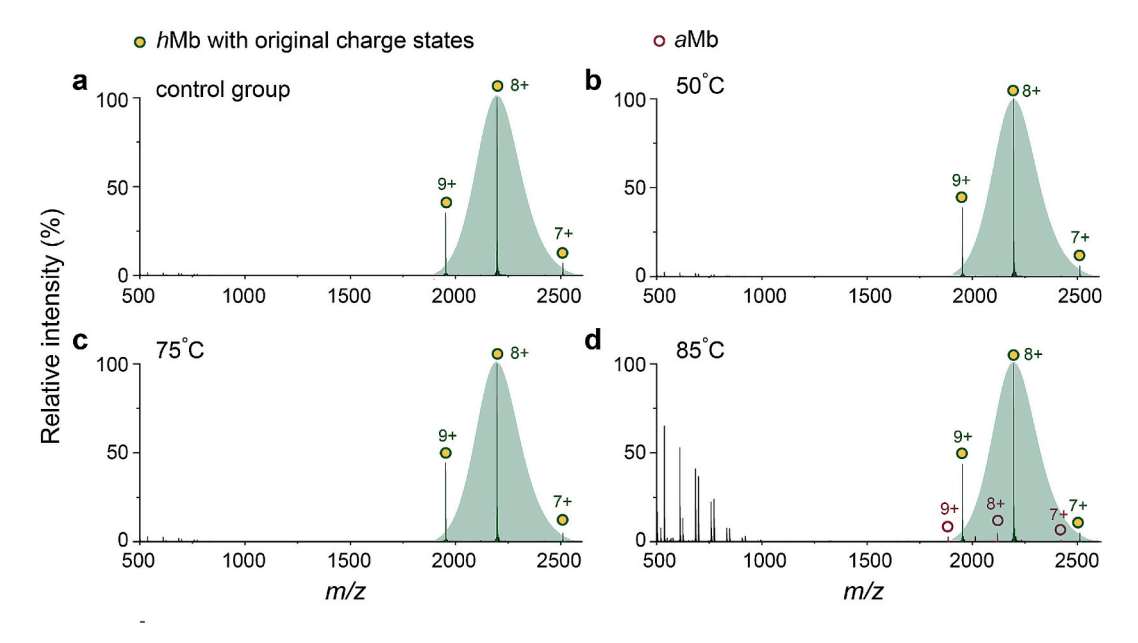


Fig. 1. nMS spectra of Mb acquired at different ESI conditions.

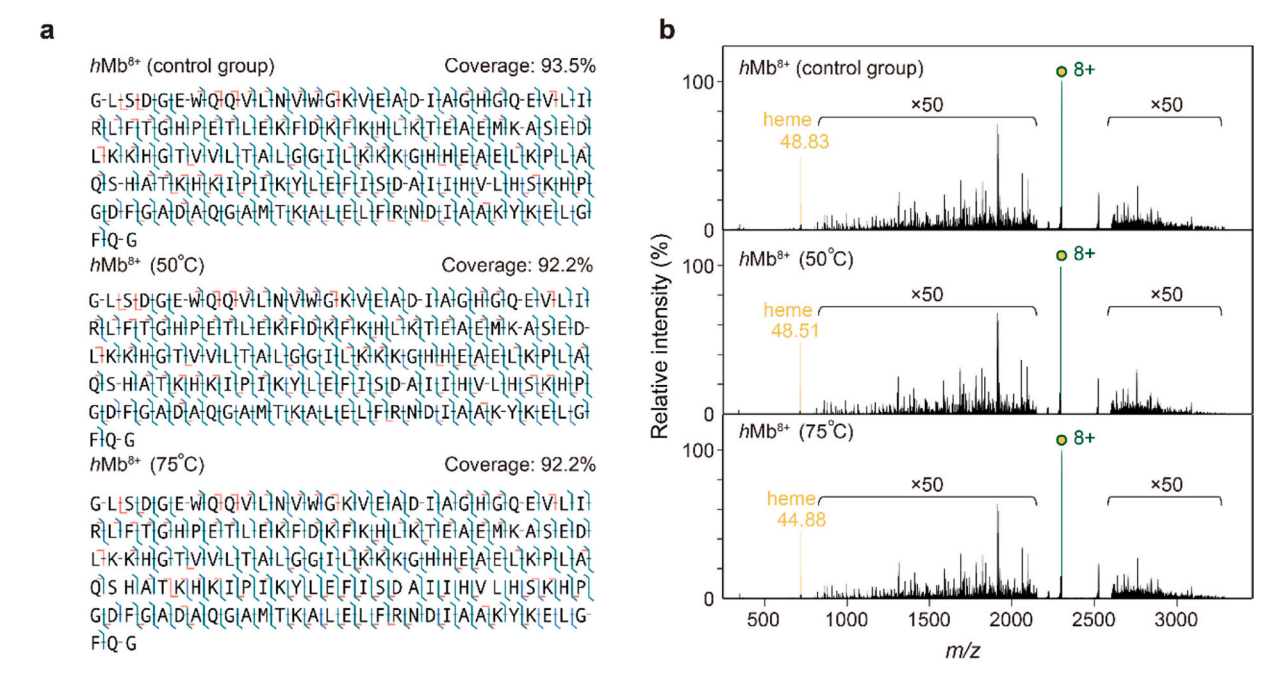


Fig. 2. (a) the coverage maps and (b) the MS/MS spectra of hMb^{8+} ionized from different solutions in 193-nm UVPD analysis.

significant tertiary structure unfolding after 50 °C or 75 °C heating treatments. Consecutive regions with decreased FYs were observed for residues E59 - G65 in helix E, A90 - H93 in helix E after 50 °C heat treatment, and residues K42 - K47 in helix E, K62 - G65 in helix E after 75 °C heat treatments. Interestingly, most of residues with decreased FYs were located in the heme-binding pocket, indicating the intramolecular interactions in the heme-binding pocket were strengthened and regions surrounding the ligand even refolded into a more stable conformation. Significantly, the FYs of H64 decreased as the temperature rose from 50 °C to 75 °C, suggesting that the H64 local interactions were further strengthened. Moreover, the significant increase in H64 interactions finally induced the formation of a double coordination between H93/H64 and heme upon 75 °C heat treatment, as reflected by the significant decrease of released heme ions in UVPD spectra. The integration of nMS

and UVPD techniques in this study highlights their utility in assessing the thermal stability and elucidating the related molecular mechanisms.

3.3. Molecular dynamics simulations at different temperatures

We also performed MD simulations of hMb at 298 K and 348 K (Fig. 4). The root mean square deviation (RMSD) of Mb backbone heavy atoms were computed along with trajectories and were found to remain below 1.2 Å (Fig. 4a), suggesting that the tertiary structure of the protein has not changed much. However, discrepancies observed in the UVPD fragmentation data hinted at alterations in the intramolecular interactions, prompting us to investigate these interactions further, particularly focusing on hydrogen bonds (H-bonds). Statistical analysis indicated that the frequency of H-bond formation between heme and Mb

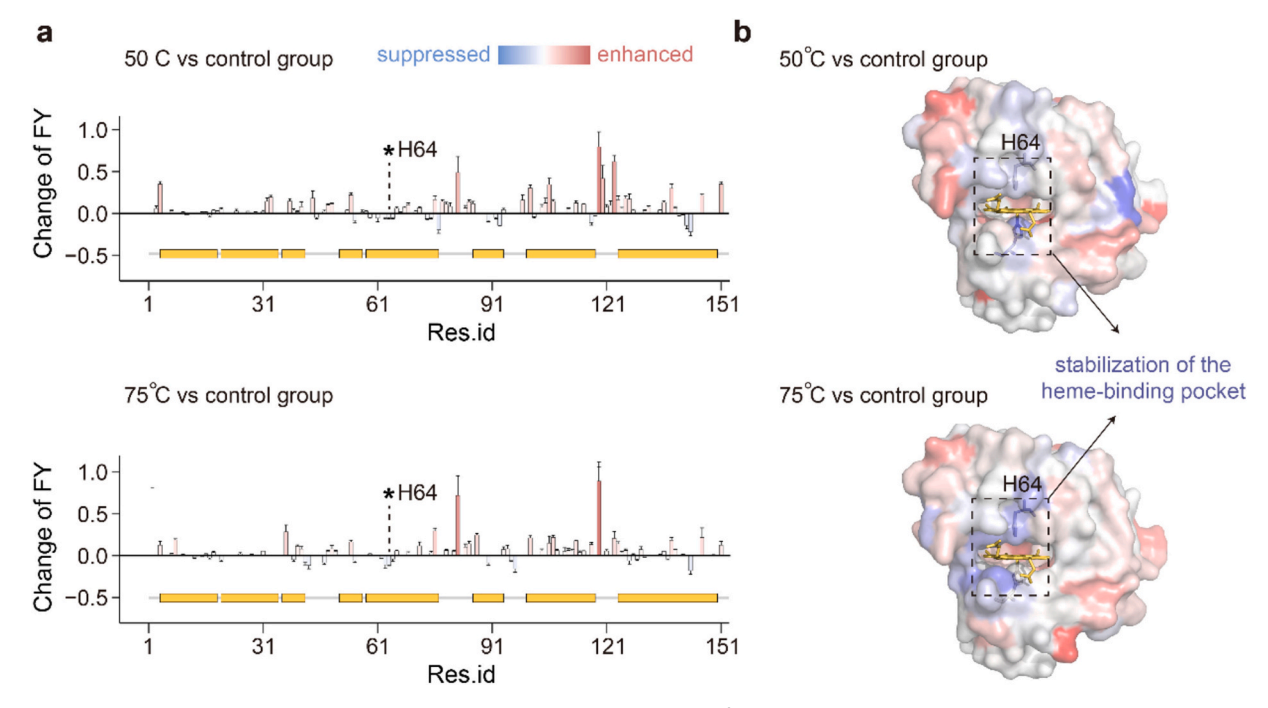


Fig. 3. (a) The alterations of residue FYs with significant differences (p value <0.05) of hMb⁸⁺ ionized from different solutions in 193-nm UVPD analysis and (b) the results were mapped to the crystal structure (PDB: 1dwr).

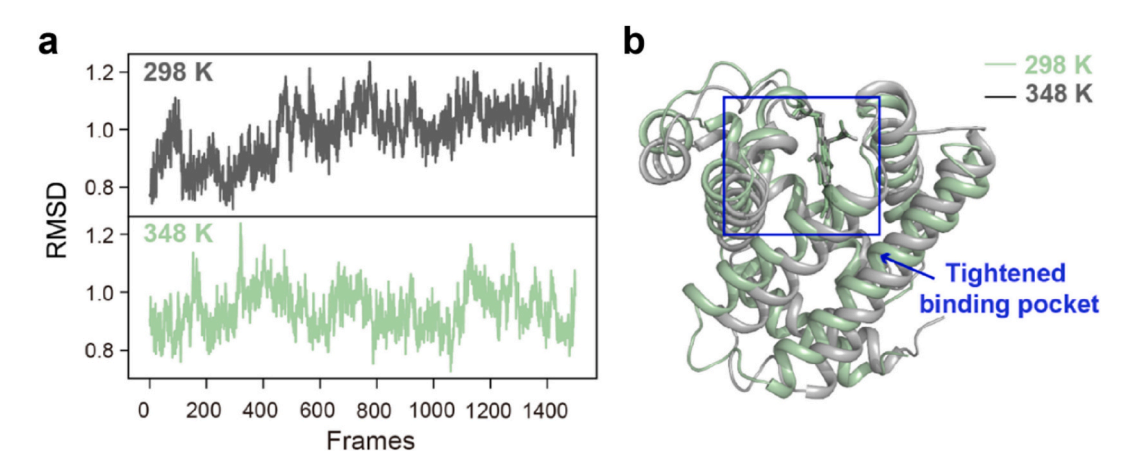


Fig. 4. (a) RMSD change curve of Mb backbone heavy atom and (b) the representative conformations in MD simulations at 298 K and 348 K.

was higher at 348 K compared to 298 K (Table S1), consistent with the enhanced binding affinity observed in UVPD. Interestingly, H64 might also participate in coordinating with the heme group at elevated temperatures, similar to the hypothesis proposed by Olson et al. [24]. We computed the average distances between the nitrogen atom in H64's side chain and the iron atom in the heme group (Table S2) and confirmed that H64 was closer to the heme at higher temperatures. This finding supports the possibility of a double coordination between H93/ H64 and heme at 348 K, which could contribute to a more stable binding pocket. We also performed cluster analysis on the conformations derived from the MD simulation trajectories. The representative conformations obtained from the analysis showed a tightened binding pocket, which corroborated with the experimental observations (Fig. 4b). Overall, these findings supported the conclusion that elevated temperatures led to the formation of new intermolecular interactions, resulting in a more compact heme-binding pocket and reduced heme ion release.

4. Conclusion

In this paper, nMS and UVPD were used for an integrated strategy to characterize the thermal stability of Mb and elucidate the in-solution conformation dynamics. nMS analysis revealed that heat treatment above T_m induced irreversible damage to the overall conformation of proteins, as reflected by the significant decrease in MS signal. In contrast, Mb maintained the overall structural integrity below T_m while the stabilization of the heme-binding pocket was observed. MD simulation results at 298 K and 348 K were consistent with the UVPD results. This work established a high-throughput analytical platform for assessing the thermal stability of proteins.

CRediT authorship contribution statement

Pan Luo: Writing – original draft, Project administration, Investigation. Dai Zhang: Writing – original draft, Investigation. Jin Liu: Investigation. Yue Xuan: Investigation. Haoxin Fan: Investigation. Jieying Xue: Investigation. Zheyi Liu: Writing – review & editing, Data

curation, Conceptualization. **Fangjun Wang:** Writing – review & editing, Conceptualization.

Declaration of competing interest

The authors declare that they have no known competing financial interests or personal relationships that could have appeared to influence the work reported in this paper.

Acknowledgements

We acknowledged the financial supported by the National Key Research and Development Program of China (2022YFA1304601), National Natural Science Foundation of China (No. 32088101, 92253304, 22288201, 22404115), the Strategic Priority Research Program of the Chinese Academy of Sciences (XDB0970100) and the grants from DICP (DICP I202242, DICP I202228). We thank the staff members of the Biological Mass Spectrometry System (https://cstr.cn/31127.02.DCLS. ESBMS) at the Dalian Coherent Light Source (https://cstr.cn/31127.02.DCLS), for providing technical support and assistance in data collection and analysis.

Appendix A. Supplementary data

Supplementary data to this article can be found online at https://doi.org/10.1016/j.cplett.2025.142294.

Data availability

Data will be made available on request.

References

- [1] J.O. Wrabl, J. Gu, T. Liu, T.P. Schrank, S.T. Whitten, V.J. Hilser, The role of protein conformational fluctuations in allostery, function, and evolution, Biophys. Chem. 159 (2011) 129–141.
- [2] D.E. Clemmer, D.H. Russell, E.R. Williams, Characterizing the conformationome: toward a structural understanding of the proteome, Acc. Chem. Res. 50 (2017) 556–560.
- [3] S. Tamara, M.A. den Boer, A.J.R. Heck, High-resolution native mass spectrometry, Chem. Rev. 122 (2022) 7269–7326.
- [4] A.D. Rolland, J.S. Prell, Approaches to heterogeneity in native mass spectrometry, Chem. Rev. 122 (2022) 7909–7951.
- [5] H.-Y. Yen, I. Liko, W. Song, P. Kapoor, F. Almeida, J. Toporowska, K. Gherbi, J.T. S. Hopper, S.J. Charlton, A. Politis, M.S.P. Sansom, A. Jazayeri, C.V. Robinson, Mass spectrometry captures biased signalling and allosteric modulation of a G-protein-coupled receptor, Nat. Chem. 14 (2022) 1375–1382.
- [6] Y. Bai, Z. Liu, Y. Li, H. Zhao, C. Lai, S. Zhao, K. Chen, C. Luo, X. Yang, F. Wang, Structural mass spectrometry probes the inhibitor-induced allosteric activation of CDK12/CDK13-cyclin K dissociation, J. Am. Chem. Soc. 145 (2023) 11477–11481.
- [7] A.O. Oluwole, R.A. Corey, C.M. Brown, V.M. Hernandez-Rocamora, P.J. Stansfeld, W. Vollmer, J.R. Bolla, C.V. Robinson, Peptidoglycan biosynthesis is driven by lipid transfer along enzyme-substrate affinity gradients, Nat. Commun. 13 (2022).

- [8] S. Chen, T. Getter, D. Salom, D. Wu, D. Quetschlich, D.S. Chorev, K. Palczewski, C. V. Robinson, Capturing a rhodopsin receptor signalling cascade across a native membrane, Nature 604 (2022) 384–390.
- [9] R. Grandori, Origin of the conformation dependence of protein charge-state distributions in electrospray ionization mass spectrometry, J. Mass Spectrom. 38 (2003) 11–15.
- [10] J.S. Brodbelt, L.J. Morrison, I. Santos, Ultraviolet photodissociation mass spectrometry for analysis of biological molecules, Chem. Rev. 120 (2020) 3328–3380.
- [11] M. Sharon, How far can we go with structural mass spectrometry of protein complexes? J. Am. Soc. Mass Spectrom. 21 (2010) 487–500.
- [12] J.L.P. Benesch, B.T. Ruotolo, F. Sobott, J. Wildgoose, A. Gilbert, R. Bateman, C. V. Robinson, Quadrupole-time-of-flight mass spectrometer modified for higher-energy dissociation reduces protein assemblies to peptide fragments, Anal. Chem. 81 (2009) 1270–1274.
- [13] H. Zhang, W. Cui, J. Wen, R.E. Blankenship, M.L. Gross, Native electrospray and electron-capture dissociation FTICR mass spectrometry for top-down studies of protein assemblies, Anal. Chem. 83 (2011) 5598–5606.
- [14] J.P. O'Brien, W. Li, Y. Zhang, J.S. Brodbelt, Characterization of native protein complexes using ultraviolet photodissociation mass spectrometry, J. Am. Chem. Soc. 136 (2014) 12920–12928.
- [15] M.B. Cammarata, R. Thyer, J. Rosenberg, A. Ellington, J.S. Brodbelt, Structural characterization of dihydrofolate reductase complexes by top-down ultraviolet photodissociation mass spectrometry, J. Am. Chem. Soc. 137 (2015) 9128–9135.
- [16] S.N. Sipe, E.B. Lancaster, J.P. Butalewicz, C.P. Whitman, J.S. Brodbelt, Symmetry of 4-oxalocrotonate tautomerase trimers influences unfolding and fragmentation in the gas phase, J. Am. Chem. Soc. 144 (2022) 12299–12309.
- [17] L. Zhou, Z. Liu, Y. Guo, S. Liu, H. Zhao, S. Zhao, C. Xiao, S. Feng, X. Yang, F. Wang, Ultraviolet photodissociation reveals the molecular mechanism of crown ether microsolvation effect on the gas-phase native-like protein structure, J. Am. Chem. Soc. 145 (2023) 1285–1291.
- [18] X. Chen, S. Ji, Z. Liu, X. Yuan, C. Xu, R. Qi, A. He, H. Zhao, H. Song, C. Xiao, W. Gao, P.R. Chen, R. Luo, P. Li, F. Wang, X. Yang, R. Tian, Motif-dependent immune co-receptor interactome profiling by photoaffinity chemical proteomics, Cell Chem. Biol. 29 (2022) 1024–1036.
- [19] P. Luo, Z. Liu, C. Lai, Z. Jin, M. Wang, H. Zhao, Y. Liu, W. Zhang, X. Wang, C. Xiao, X. Yang, F. Wang, Time-resolved ultraviolet photodissociation mass spectrometry probes the mutation-induced alterations in protein stability and unfolding dynamics, J. Am. Chem. Soc. 146 (2024) 8832–8838.
- [20] S. Yang, Z. Hou, Z. Liu, Z. Jin, H. Zhao, K. Cao, S. Zhao, W. Zhang, C. Xiao, X. Yang, G. Huang, F. Wang, In-cell mass spectrometry and ultraviolet photodissociation navigates the intracellular protein heterogeneity, J. Am. Chem. Soc. 147 (2025) 4714–4719.
- [21] M.C. Chambers, B. Maclean, R. Burke, D. Amodei, D.L. Ruderman, S. Neumann, L. Gatto, B. Fischer, B. Pratt, J. Egertson, K. Hoff, D. Kessner, N. Tasman, N. Shulman, B. Frewen, T.A. Baker, M.-Y. Brusniak, C. Paulse, D. Creasy, L. Flashner, K. Kani, C. Moulding, S.L. Seymour, L.M. Nuwaysir, B. Lefebvre, F. Kuhlmann, J. Roark, P. Rainer, S. Detlev, T. Hemenway, A. Huhmer, J. Langridge, B. Connolly, T. Chadick, K. Holly, J. Eckels, E.W. Deutsch, R. L. Moritz, J.E. Katz, D.B. Agus, M. MacCoss, D.L. Tabb, P. Mallick, A cross-platform toolkit for mass spectrometry and proteomics, Nat. Biotechnol. 30 (2012) 918–920.
- [22] Q. Kou, L. Xun, X. Liu, TopPIC: a software tool for top-down mass spectrometrybased proteoform identification and characterization, Bioinformatics 32 (2016) 3495–3497.
- [23] D.W. Woodall, L.W. Henderson, S.A. Raab, K. Honma, D.E. Clemmer, Understanding the thermal denaturation of myoglobin with IMS-MS: evidence for multiple stable structures and trapped pre-equilibrium states, J. Am. Soc. Mass Spectrom. 32 (2021) 64-72.
- [24] D.S. Culbertson, J.S. Olson, Role of heme in the unfolding and assembly of myoglobin, Biochemistry 49 (2010) 6052–6063.